JOURNAL OF ZOOLOGICAL SYSTEMATICS AND EVOLUTIONARY RESEARCH

Mandible size and shape in extant Ursidae (Carnivora, Mammalia): a tool for taxonomy and ecogeography

Abstract:	The family Ursidae is currently one of the taxonomic group with the lowest number of species among Carnivora. Extant bear species exhibit broad ecological adaptations both at inter and intra specific level and taxonomic issues within this family remain unresolved (i.e. the number of recognisable subspecies). Here, we investigate a sample of bear mandibles using two-dimensional geometric morphometrics to better characterise bear taxonomy and evolution with a focus on one of the most widespread species: the brown bear (Ursus arctos). Our analyses confirm that both size and shape data are useful continuous characters that discriminate with very high percentage of accuracy extant bears. We also identify two very distinct mandibular morphologies in the subspecies Ursus actos isabellinus and Ursus arctos marsicanus. These taxa exhibit a high degree of morphological differentiation possibly as a result of a long process of isolation. Ecogeographical variation occurs among bears mandibles with climate strongly impacting the diversification of the whole family.

Title: **Mandible size and shape in extant Ursidae (Carnivora, Mammalia): a tool for taxonomy and ecogeography**

Authors: Carlo Meloro[1], Giulia Guidarelli[2], Paolo Colangelo[3], Paolo Ciucci[4], Anna Loy[2]

Addresses: [1]*Research Centre in Evolutionary Anthropology and Palaeoecology, School of Natural Sciences and Psychology, Liverpool John Moores University, Byrom Street, Liverpool L3 3AF, UK. Phone: +44 01512312312; Fax number: +44 01517 099864*

[2]*Department S.T.A.T., University of Molise, I-86090 Pesche, Italy. Phone: +39 0874404140; Fax number: + 39 0874 404 814*

[3]*CNR - Institute for Ecosystem Study, Verbania-Pallanza, Italy. Phone: +39 06 49918122; Fax number: +39 0323 556513*

[4]*Department of Biology and Biotechnologies 'Charles Darwin', University of Rome 'La Sapienza', Roma, Italy. Phone: +39 0649914750; Fax number: +39 0649912351*

Corresponding author: Carlo Meloro (C.Meloro@ljmu.ac.uk)

Contributing authors: Giulia Guidarelli (g.guidarelli@studenti.unimol.it); Paolo Colangelo (paolo.colangelo@uniroma1.it); Paolo Ciucci (paolo.ciucci@uniroma1.it); Anna Loy (a.loy@unimol.it)

Abstract

The family Ursidae is currently one of the taxonomic group with the lowest number of species among Carnivora. Extant bear species exhibit broad ecological adaptations both at inter and intra specific level and taxonomic issues within this family remain unresolved (i.e. the number of recognisable subspecies). Here, we investigate a sample of bear mandibles using two-dimensional geometric morphometrics to better characterise bear taxonomy and evolution with a focus on one of the most widespread species: the brown bear (*Ursus arctos*). Our analyses confirm that both size and shape data are useful continuous characters that discriminate with very high percentage of accuracy extant bears. We also identify two very distinct mandibular morphologies in the subspecies *Ursus actos isabellinus* and *Ursus arctos marsicanus*. These taxa exhibit a high degree of morphological differentiation possibly as a result of a long process of isolation. Ecogeographical variation occurs among bears mandibles with climate strongly impacting the diversification of the whole family.

Key Words: Bears − geometric morphometrics – morphology − Discriminant Function Analysis − Partial Least Squares

Introduction

The family Ursidae comprises powerful and large terrestrial members of the mammalian order Carnivora that evolved in the northern hemisphere and are currently distributed in Eurasia, North Africa and the Americas (Herrero 1999). Despite the relatively low taxonomic diversity within the family, the eight extant species show a remarkable variation in ecology and behaviour that allowed them to colonize a broad range of environments from the tropical rainforest to the extreme arctic ice sheets. As for feeding ecology, the majority of bear species exhibit an omnivorous diet with the exception of the highly carnivorous polar bear (*Ursus maritimus* Phipps, 1774) and other extreme forms of dietary specialisation reported for the bamboo feeder giant panda (*Aiuloropoda melanoleuca* David, 1869) and the insectivorous sloth bear (*Melursus ursinus* Shaw, 1791) (Herrero 1999).

Extant bears are morphologically distinct from the other Carnivora for being large in body size (Ewer 1973; Gittleman 1985). They exhibit big skulls with developed crushing molars and reduced premolar regions (in both upper and lower jaws). Morphological variation between ursids apparently reflects their feeding ecology with this being especially true for the mandible (Mattson 1998; Sacco and Van Valkenburgh 2004; Meloro 2011; Meloro and O'Higgins 2011; Figueirido et al. 2009; van Heteren et al. 2009, 2014, 2016). Herbivorous bears, including the giant panda and the South American Andean bear (*Tremarctos ornatus* Cuvier, 1825), are characterised by a tall ramus mandibulae for the attachment of the temporalis muscle complex and an enlarged posterior portion of the mandibular body (Meloro 2011; van Heteren et al. 2016). The insectivore *Melursus ursinus* shows a smaller ramus, lower coronoid and a more curved mandibular profile (van Heteren et al. 2016) while the majority of omnivorous bears have a more developed diastema and their mandibular body is homogeneously thick at the front and posterior areas (Meloro 2011). Such characteristics reflect ecological adaptations but they also allow characterising bear taxonomy

in more details. Van Heteren et al. (2016) recently reported a significant phylogenetic signal in mandibular shape data also after allometric differences were removed and size morphological changes are equally expected to inform bear taxonomy.

Due to the broad geographic distribution of many bear species, it is likely that mandibular morphology might change across geographical areas even within the same species. Changes in skull morphometry have been reported for the brown (*Ursus arctos* Linnaeus, 1758) and American black bear (*Ursus americanus* Pallas, 1780) in relation to their geographical range (Rausch 1963; Byun et al. 1997; Kennedy et al. 2002) and the same applies to the Malayan bear (*Helarctos malayanus* Raffles, 1821) (Meijaard 2004). Kitchener (2010) highlighted the need of investigating more in details bear morphological variation to clarify aspects in relation to their taxonomy and conservation. Here, we aim to focus on mandibular size and shape of extant bears to inform species taxonomy and ecogeography with a particular focus on the brown bear.

Among the eight species, the brown bear is the most widely distributed having a circumpolar distribution that includes a variety of habitats with different environmental conditions. This species shows an extremely seasonal and opportunistic diet that varies significantly throughout its range according to climatic and biotic conditions, i.e. productivity and type of biome (Bojarska and Selva 2012). Although globally the population remains large (McLellan et al. 2008), the brown bear range has dramatically reduced and disappeared from many areas as a consequence of human persecution and habitat destruction. Now the largest populations are limited to North America (Alaska and Canada), Russia and to the Carpathian and Dinaric Mountains, while in South Asia and Western Europe populations are small and isolated. In Western Europe the remaining populations of the Cantabrian Mountains, Pyrenees, Eastern Alps and Apennines are extremely small, isolated and seriously endangered (Zedrosser et al. 2001). Wilson and Reeder (2005) recognized 14 subspecies of

U. arctos, seven of which are distributed in North America, one in Europe, three in Central Asia and three in Eastern Asia. Because of the considerable morphological variation within the species, there is great disagreement regarding the taxonomy of North American populations which, so far, have been grouped into two (Rausch 1963) to seven (Hall 1981) subspecies, based on morphology only. For Eurasian brown bears there are not many morphological studies focusing on subspecies description (Baryshnikov et al. 2004; Mihaylov et al. 2013) with few of them using updated morphometric approaches to highlight distinctiveness of the endangered Apennine subspecies, *U. arctos marsicanus* Altobello, 1921 (Loy et al. 2008; Colangelo et al. 2012) .

The proliferation of molecular studies (Waits et al. 1999; Barnes et al. 2002; Calvignac et al. 2008; Krause et al. 2008) is to some extent counterbalancing the lack of useful information on bear taxonomy, but they are also questioning in many cases previous morphological findings. All bears are at risk of extinction and are listed as Vulnerable in the IUCN red list (IUCN 2016), except the brown bear and the American black bear that are of Least Concern (McLellan et al. 2008; Garshelis et al. 2008c). Uncertainty in their taxonomy might have negative consequence for conservation planning, both in the wild (i.e., define the ideal source populations for restocking or reintroductions) and in captivity (i.e., captive breeding programs), especially when dealing with wide ranging species. The success of conservation programs might be compromised by outbreeding depression derived from outcrossing between inconsistent subspecies (Banes et al 2016). A more adequate prospect on bear conservation could be obtained by a combined molecular and morphological approach (Cronin 1993).

We apply 2D geometric morphometrics (Adams et al. 2004, 2013) to study patterns of mandibular morphological variation within the family Ursidae. We present three analytical steps to narrow taxonomic variation in bears' mandible: 1) interspecific comparison among

the eight species; 2) interspecific variation within the genus *Ursus*; 3) intraspecific variation within the species *U. arctos*. Our aim is to characterize taxonomic distinctiveness as revealed by mandibular morphology at both inter and intraspecific scale especially for the widely distributed brown bear, by taking into account ecogeographical differentiation (Cardini et al. 2007; Cáceres et al. 2014; Meloro et al. 2014a, b).

Materials and Methods

Sample size

Size and shape data were collected on 169 mandibles belonging to the eight extant species from different areas of their range (Appendix 1, Table S1). Only adult specimens were selected according to museum record and tooth eruption. Mandibles were photographed in lateral view using a Nikon 3100 digital camera placed on a tripod at a minimum 1m distance. Mandibles were positioned on the floor and a spirit level was placed on them to ensure parallelism with the camera plane. We digitized fourteen 2D landmarks generally on the right lateral mandibular side (Fig. 1) using the software TpsDig2 (Rohlf 2015). Landmarks were selected to record main positioning of canine, lower p4, carnassial slicing area and molar crushing area as well as ramus, coronoid and condyle. Previous investigations supported this configuration for being informative both ecologically and taxonomically in Carnivora as well as Ursidae (see Meloro 2011, 2012; Meloro and O'Higgins 2011; Figueirido et al. 2009). Although 3D landmarking might provide more detailed information on mandibular size and shape (see van Heteren et al. 2016; Fuchs et al. 2015), a recent work by Cardini (2015) demonstrated that results between 2D and 3D morphometrics are generally congruent when concerning mammalian mandibles thus allowing substantial generalisation to be valid at all

scales of biological variation. For species and subspecies taxonomic identification, we followed museum specimen labels and applied nomenclature proposed by Kitchener (2010).

Geometric morphometrics

A Generalized Procrustes Analysis (GPA) was performed to translate, rotate and scale the landmark configuration of each specimen to a unit centroid size (=CS; a proxy for size of landmark configuration defined as the square root of the summed squared distances of all landmarks to the centroid, Bookstein 1989). GPA removes all the information unrelated to shape and superimposes the objects in a common coordinate system (Rohlf and Slice 1990): the new set of coordinates are named Procrustes and they define the multivariate shape space, while the centroid size values are stored as a measure of size (Zelditch et al. 2004). Statistical analyses on shape variables were conducted on three levels: 1) interspecific variation in the whole family Ursidae (169 specimens); 2) interspecific variation within the genus *Ursus* (119 specimens); intraspecific variation within the species *U. arctos* (78 specimens).

On each sample Procrustes coordinates were firstly decomposed into affine and non-affine components of the bending energy matrix and then subjected to principal component analysis setting the exponential weight alpha to zero (named also relative warp analysis RWA, Rohlf 2000). This allows visualisation of shape differences from the mean using thin plate spline through the tpsRelw package (Rohlf 2015).

Taxonomic and sexual differences in shape were tested employing Procrustes ANOVA as implemented in the R package geomorph (Adams and Otárola-Castillo 2013; Adams and Collyer 2015). A 9,999 permutation test on full factorial models inclusive of the interaction factor term (i.e., taxonomy x sex) was performed. Differences in mandibular size due to taxonomy or sex were similarly tested by using standard ANOVA followed by post-hoc tests (Meloro and O'Higgins 2011).

Discriminant function analyses (DFA) were subsequently performed using shape coordinates and lnCS as predictor variables of taxonomic categorisation (species or subspecies depending on the level). A forward stepwise method was applied allowing the selection of the only predictive variables and a leave-one-out procedure was run to validate the results of the discriminant functions. Single variables were added to optimize discrimination among taxonomic categories (species or subspecies) with an inclusive criteria of F probability values greater than or equal to 0.05. Variables excluded from the discriminant model do not pass the F value threshold with $P \geq 0.10$. Shape variation along discriminant function axes was visualized by regressing discriminant function scores on shape variables with the software tpsRegr v. 1.34 (Rohlf 2015). This methodology proved to be robust in relation to group size and variable numbers (see Meloro 2011; Meloro et al. 2015a). It is also useful to provide visualisation of shape differences and classify specimens with unknown categorisation (this being the case for some brown bear specimens in our sample whose subspecies and geographic location were unknown).

Unweighted Pair Group Method with Arithmetic Mean (=UPGMA) cluster analyses were also performed based on averaged Procrustes distances obtained for species or subspecies in order to identify cophenetic similarities between pre-determined taxonomic groups. A molecular phylogeny of bear species was generated using the 10K tree project database (Arnold et al. 2010) to provide a comparative baseline for the UPGMA trees. Although different phylogenetic trees are available for extant and fossil bears (e.g., Pagès et al. 2008), we used the 10K project to extract a consensus topology with branch lengths (time of divergence in millions years) that is entirely based on the most updated molecular datasets, statistically treated using Bayesian phylogenetics. Aim of these analyses was to identify taxonomic signal that might be coherent or not with current bear phylogenetic hypotheses (Cardini and Elton 2008). In addition, the recently developed K_{multiv} statistic (Adams 2014)

was quantified based on the interspecific dataset of mandible shape ($N = 8$) using the package geomorph (Adams and Otárola-Castillo 2013). K_{multiv} is an extension of the K statistic introduced by Blomberg et al. (2003) to measure the strength of phylogenetic signal. A K close or bigger than 1 demonstrates that phenotypic differences between species followed a pattern expected by Brownian motion of evolution. Value of K similar to zero occurs if phenotypic trait evolved according to a star phylogeny (that is: no phylogenetic signal is present in the data).

Ecogeographical variation

In order to explore ecogeographical variation within our sample (Cardini et al. 2007; Meloro et al. 2014a, b; Bubadué et al. 2016), we recorded geographic collection localities every time they were available (69 out 169 specimens). When broad geographic information was available (i.e., Alaska, Peru), we used the species' distribution map to approximate a centroid locality within the species range (see also Meloro et al. 2013). With this procedure, longitudinal and latitudinal data became available for a subsample of 130 specimens distributed across 75 localities. If multiple specimens belonged to the same locality or to locations that changed only of few decimal seconds (<30), their landmark configurations were averaged to avoid pseudo-replications. Nineteen bioclimatic variables (see Appendix 2 for a full description) were extracted for the 75 localities and standardised as a proxy for climate with a resolution of 10 seconds from the WorldClim raster database (Hijmans et al. 2005) by using DIVA-GIS 7.5 software (http://www.diva-gis.org/download). Partial Least-Squares (PLS) was employed to identify any possible covariation between mandible shape and climate (Rohlf and Corti 2000). PLS employs a singular value decomposition (SVD) to generate orthogonal vectors (the singular axes, SA) which account for the maximum amount of covariation between the two sets of variables. A singular value (SV) is associated to each

pair of axes and expresses the amount of covariance they account for (Zelditch et al. 2004). Aim of this approach was to test for the impact of climate on taxonomic differentiation at both inter and intra generic scale (Cáceres et al. 2014; Meloro et al. 2014a, b; Bubadué et al. 2016). If climate strongly influences mandible shape in Ursidae, their taxonomy should also take local adaptations into account as well as geographic isolation.

To better characterize mandibular shape variation within our sample, a variation partitioning approach was also applied using shape variables as response and climate (continuous standardised variables inclusive of all the 19 bioclim), taxonomy (categorical variable), sex and size (continuous variable, ln CS) as explanatory variables (Cardini et al. 2007; Meloro et al. 2014a, b; Cáceres et al. 2016). Variation partitioning allows testing for contribution of climate, size, sex, and taxonomic categorisation on mandibular shape variance, taking their interaction into account. In order to take also the impact of sexual dimorphism into account, we used for this analysis a subsample of 66 specimens for which geographic location was available. In this case, specimens were not averaged by geographic location to maximise sample size and include intraspecific sexual variation (Cáceres et al. 2016). This analysis was performed using the R package vegan (Oksanen et al. 2012).

Results

Ursidae

Interspecific mandibular shape differences

Relative warp analysis of mandible shape showed variance to be quite spread across relative warp (=RW) vectors of which the first 12 explained altogether 95% of the total variance (=var.). The scatterplot of RW1 (23.56% var.) vs RW2 (19.87% var.) showed a good

separation of *A. melanoleuca* and *M. ursinus* respectively on the negative and positive extreme of the RW1, while the second RW detected good discrimination for the giant panda on positive scores (Fig. 2A). The other bear species overlapped in the central region of the plot with *H. malayanus* showing more positive RW2 scores than *Ursus* spp.. RW1 described main shape changes in the relative height of the mandibular ramus, the position of molar crushing region, the diastema and the relative corpus thickness. On the RW2 species could be distinguished by the position of lower fourth premolar, molar crushing region, relative height and width of the ramus and corpus thickness.

The Procrustes ANOVA showed taxonomy as a significant factor explaining 56% of the shape variance (SS = 0.516, MS = 0.073, R² = 0.558, F = 29.114, p < 0.001). A non-parametric MANOVA based on 28 Procrustes coordinates confirmed this (Tot SS = 0.9379, Within-group SS = 0.4158, F = 28.88, p < 0.001) and, after pairwise comparisons based on Euclidean distances, all species differed from each other, except when Bonferroni correction was applied. In this case the only non-significant pair was *U. americanus* /*U. arctos* (p > 0.1). When sexual dimorphism is concerned the sample was reduced to 74 mandibles. Sex alone explained c.ca 3.5% of mandibular shape variance (SS = 0.011, MS = 0.011, R² = 0.035, F = 2.644, p = 0.013). A more complex model including both species and sex as factor showed that no interaction occurred between the two (Table 1).

Size and allometry

Size (lnCS) differed significantly among species (F = 31.537, df = 7, 161, p < 0.0001; Fig. 3), with post hoc tests supporting *T. ornatus* and *H. malayanus* as the most distinctive compared to the other species (Table S2). The brown bear was also distinct in size and it overlapped with the polar bear only (Table S2). Sex was a significant factor in mandibular size variation (74 mandibles) and it explained about 7% of variance (SS = 0.272, MS = 0.272, R² = 0.071, F

= 5.531, p = 0.023). The ANCOVA model demonstrated that sexual dimorphism in size did not interact with species taxonomic differences as it applied for shape data (Table 1).

A significant allometric impact occurred on mandible shape, with size explaining 6.9% of the variance (F = 12.431, P < 0.0001). Deformation grids showed from small to large specimens a shrink in the premolar region and in the mandibular body with large taxa such as the polar bear exhibiting a long and slender mandible with broad expansion of the diastema (Fig. 3). Procrustes ANCOVA also evidenced no significant interaction between size and species (SS = 0.01922, MS = 0.002745, R² = 0.0208, F = 1.1323, p = 0.9987).

Discriminant function analysis

The Discriminant Function Analysis run on the whole sample (169 individuals) with Procrustes coordinates and lnCS as predictors extracted seven statistically significant discriminant functions (DF) loaded on 20 variables including centroid size. A combination of the first three discriminant functions (85% of cumulative var.) showed strong separation in the morphospace among species (Fig. 2B), supported by the high percentage of correctly classified cases after jackknifing (92.3% Total). The functions provided 100% of correct classification for the panda, the Malayan bear, the sloth bear, and the Andean bear. *U. arctos* and *U. maritimus* were classified with 92.3 and 90.9% of accuracy respectively while the Tibetan bear and American black bear had lower rates (85.2 and 75.0%, respectively).

The first discriminant axis (54.1% var.; Wilk's lambda = 0.000024; Chi-Square = 1637.413, df = 140; p < 0.0001) was loaded on landmarks that describe the premolar region as well as the molar slicing area and the ramus. The giant panda occupied the most negative DF1 scores and it was characterised by a tall ramus, longer slicing molar area and premolar region and a thinner corpus. On positive DF1 scores the Malayan bear can be distinguished due to its short and thick corpus and low mandibular ramus. On DF2 (17.4% var.; Wilk's lambda = 0.001;

Chi-Square = 1147.58, df = 114; p < 0.0001) a strong deformation in the molar area and a higher ramus distinguished the panda and the Malayan bear from the other taxa. The third DF (13.6% var.; Wilk's lambda = 0.005; Chi-Square = 819.526, df = 140; p < 0.0001) separated the polar and the brown bear from the Andean bear, the panda and the Malayan bear loading again on premolar region and molar slicing area. This axis also correlated negatively with centroid size (r = -0.368) so that specimens with positive scores are smaller than the one with negative scores.

Genus *Ursus*

In these analyses, we considered brown bear's subspecies as distinct groups, so the sample was reduced from 169 to 119. In order to test for the impact of species and subspecies (for the brown bear only) differences, the sample of *Ursus* specimens was reduced from 119 (as showed in the RWA) to 114 because subspecies classification was not available for five specimens of *U. arctos*. Similarly, to test for the impact of sex, the sample size was reduced to 53 sexed specimens.

Inter and intraspecific mandibular shape differences

RWA extrapolated 24 axes of which the first 14 explained almost 95% of the total variation. A plot of RW1 (21.98% var.) vs RW2 (17.31% var.) showed strong overlap between all subspecies of brown bear and the American black bear (Fig. 4A). The polar bear was distinct from the other taxa showing negative scores for both axes. The Apennine bear and the subspecies *U. arctos dalli* Merriam, 1896, also had more negative PC2 scores when compared to the other specimens. RW1 displayed a strong deformation in corpus thickness followed by an expansion of the ramus area, while RW2 was loaded on changes in the premolar region as well as in the molar slicing area. For the Procrustes ANOVA (N=114),

factor was subspecies for *U. arctos* and species for the other *Ursus* spp. Taxonomy explained quite a good portion of sample variance (32%) and differences between taxa in mandible shape were significant (SS = 0.116, MS = 0.014, R^2 = 0.321, F = 6.212, p < 0.001). This is confirmed by a non-parametric MANOVA based on 28 Procrustes coordinates (Tot SS = 0.3369, Within-group SS = 0.25, F = 6.134, p < 0.001). Pairwise comparisons based on Euclidean distances, showed significant shape differences between polar bear, Tibetan bear and all the other *Ursus* taxa (Table S3). The American black bear (*Ursus americanus*) overlaps in shape with the brown bear while the Appennine bear (*U. a. marsicanus*) and the Isabelline bear (*U. a. isabellinus*) subspecies are generally distinct from all the others. No significant shape differences occur between the North American brown bear subspecies and the Eurasiatic *U. arctos arctos* (Table S3).

Using sexed subsample of 53 specimens, sex alone explained c.ca 7% of mandibular shape variance (SS = 0.011, MS = 0.011, R^2 = 0.072, F = 3.999, p = 0.013). A more complex model including both species and sex as factors showed that significant interaction occurred between the two (Table 2).

Size and allometry

ANOVA was run on eight taxa since three *U. arctos* subspecies (*U. a. gyas* Merriam, 1902, *U. a. syriacus* Hemprich and Ehrenberg, 1828, *U. a. dalli*) could not be included due to the small sample size. Size (lnCS) was significantly different among taxa (F = 19.068; df = 8, 105, p < 0.0001) with the Tibetan bear being distinct in size from all the other taxa except the Apennine brown (*U. a. marsicanus*) and the American black bear. Among brown bear subspecies, *U. a. alascensis* Merriam, 1896, was the largest differing from every taxon except *U. a. horribilis* Ord, 1815, and *U. a. arctos* Linnaeus, 1758. The Apennine bear also differed

in size from *alascensis*, and *horribilis*. In this subsample of 114 *Ursus* specimens, size explained 5% of the shape variance (SS = 0.117, MS = 0.017, R² = 0.047, F = 5.636, p < 0.001), but the interaction between taxonomy and size as independent variables was not significant (SS = 0.02249, MS = 0.002811, R² = 0.0622, F = 1.2976, p = 0.7429).

Sex significantly influenced size variation in the *Ursus* spp. subsample explaining c.ca 13% of variance (N = 53, SS = 0.254, MS = 0.254, R² = 0.127, F = 7.391, p = 0.009). This factor also interacted significantly with taxonomy (Table 2).

Discriminant function analysis

The DFA extracted eight vectors of which the first six (98% of tot var.) were all significant. On the positive scores of DF1 (41.1% var.; Wilk's lambda = 0.001; Chi-Square = 724.833, df = 144; p < 0.0001) there was a good separation of the polar bear and the Apennine bear from the rest of the taxa being both characterised by a relatively straight corpus. DF2 (27.7% var.; Wilk's lambda = 0.006; Chi-Square = 516.243, df = 119; p < 0.0001) better characterised these species with the polar bear occupying negative scores, due to its thin corpus, and the Apennine bear positive ones with a thick and wide corpus on the anterior region. *U. a. horribilis* and the majority of other *Ursus arctos* subspecies occupied negative DF1 scores being characterised by a strongly curved mandible on the posterior area of the corpus (Fig. 4B). The Apennine brown bear subspecies together with the polar and the Tibetan bear showed rates of correct classification higher than 80% (Table 3). All the *U. arctos* subspecies without labels were categorised in all cases as *U. a. arctos*, *U. a. dalli* and *U. a. alascensis*. One of the unlabelled specimens was classified as *U. thibetanus*.

Ursus arctos subspecies

Here, the subsample employed for RWA was reduced to 78 specimens. In order to run Procrustes ANOVA models, observations were reduced to 73 to test for the impact of subspecies classification (including all the individuals with subspecies information and excluding those subspecies represented by just one specimen: *U. a. syriacus*, *U. a. gyas*) and 37 to test for the impact of sexual dimorphism.

Intraspecific mandibular shape differences

RWA of 78 *U. arctos* specimens extracted 24 RWs of which the first two accounted for the 50.85% of total variance (Fig. 5A). The Apennine brown bear was entirely distributed on RW1 positive scores and was well separated from the other subspecies. In this intraspecific context, main shape changes involved the position of the coronoid process, the most anterior point of the canine and the dorso-ventral development of the corpus that together make the mandible more convex on the positive scores of RW1.

Subspecies differed significantly in mandibular shape (SS = 0.047, MS = 0.009, R^2 = 0.229, F = 3.988, p < 0.001). When only sexed individuals are considered (N = 37) Procrustes ANOVA demonstrated that sex was a significant factor in mandibular shape differentiation and it explained c.ca 6% of shape variance (SS = 0.0056, MS = 0.0056, R^2 = 0.0591, F = 2.202, p = 0.0308). A complex model supported significant interaction between sex and taxonomy on mandible shape (Table 4).

Size and allometry

Mandibular size differed significantly between sexes with males generally larger than females and sexual dimorphism explaining 21% of size variance (N = 37, SS=0.23628, MS=0.236281 R^2=0.21385, F=9.5206, p=0.006). No interaction occurred between the factor sex and subspecies (Table 4).

Centroid size again had an impact on mandible shape but it explained only 5% of variance (SS = 0.010, MS = 0.010, R² = 0.051, F = 3.874, p < 0.005) and no interaction was detected between taxonomy and size (SS = 0.014095, MS = 0.02819, R² = 0.06737, F = 1.2419, p = 0.5209).

Discriminant function analysis

The DFA run on *U. arctos* extracted two DFs that could separate subspecies (Fig. 5B). The most divergent group was the Apennine brown bear, clearly distinguished along DF1 (60.8% of var., Wilk's lambda = 0.025; Chi-Square = 238.911, df = 40; p < 0.0001), followed by the Isabelline bear (*U. a. isabellinus* Horsfield, 1826) that was separated along DF2 (26.6% of var., Wilk's lambda = 0.145; Chi-Square = 125.30, df = 28; p < 0.0001). The Apennine bear was characterized by a convex shape of the mandible with a massive corpus and a strongly developed symphysis, while the Isabelline bear displayed a slender corpus. The other subspecies were quite superimposed on central values of both DFs, with a slight aggregation of North American subspecies (*U. a. dalli*, *U. a. horribilis*, *U. a. alascensis*). The high percentage of correctly classified cases confirmed the high success rate in discriminating the Apennine and the Isabelline subspecies but not the others (Table 3).

UPGMA and Phylogenetic Signal

By using consensus configuration for all bear species, UPGMA cluster analyses evidenced cophenetic similarities that partially followed a pattern of phylogenetic relatedness (Fig. 6A and B). The cluster obtained from mandible shape distances showed a very good cophenetic correlation (r = 0.912). The giant panda (*A. melanoleuca*) was the most distinctive in mandible shape while all *Ursus* spp. clustered together. Main differences with molecular

phylogeny were due to the position of *T. ornatus* and the American black bear that, based on mandible shape, appeared to be more similar to *Ursus* spp. and *U. arctos*, respectively (Fig. 6B). A Mantel test between the distance matrices obtained from the molecular phylogeny and the shape coordinates results in a relatively high but non-significant correlation between the two (r = 0.624; p = 0.058 after 99,999 permutations). The K_{multiv} statistic instead showed a significant phylogenetic signal in the bear mandible shape morphospace (K_{multiv} = 0.557; p = 0.032).

When only *Ursus* species were considered, the UPGMA provided a very good fit (r = 0.897) with all *Ursus arctos* subspecies clustering together (Fig. 6C). However, the American black bear showed stronger affinities with *U. arctos* North American subspecies and *U. arctos arctos*. Focusing on *U. arctos* only did not change much of the cophenetic similarity with coherent clustering between *U. a. marsicanus* and *U. a .dalli* (Fig. 6D). Still, cophenetic similarity was good (r = 0.798).

Ecogeographical variation

Partial Least Squares

In this analysis sample size was reduced from 169 to 75 averaged specimens based on geographic location. The Partial Least Squares demonstrated a strong co-variation between mandible shape and bioclimatic variables exemplified by the first pair of axes that explained 73.84% of covariation (Fig.7A). They correlated to each other strongly (r = 0.689, p < 0.001) and showed bears from colder seasonal (low Bio1-3, Bio5-6 and Bio8-11=temperature parameters, high Bio4 and Bio7=seasonality) and dry (low Bio12-13 and Bio18-19 = precipitation=) regions to be characterised by a slender mandible, thin at the corpus and on the anterior region (i.e. the polar bear). A thick corpus related to tropical environments (high

temperatures, high precipitation and lower seasonality) and was typical of taxa like the Malayan bear. In order to assess if climate impacts in the same way mandible shape variation for the genus *Ursus* only, PLS was performed separately for all non-*Ursus* taxa (non-hibernating) vs *Ursus* taxa. In non-hibernating bears only (n=19), the covariation with climate exhibited by the first pair of vectors was strong (43% of covariation, r = 0.84, p < 0.002) and significant (Fig.7B). The climatic variables that mostly showed a correlation with non-*Ursus* bear mandible shape were Bio3, 4, 5, 7, 12, 14 and 15. The sloth bear (*M. ursinus*) specimens, characterised by longer premolar region and wider coronoid, occurred in more seasonal but also warmer environments while the Malayan bear occupied wetter environments (higher precipitations) but less seasonal areas. In the genus *Ursus* (n =56) the correlation between mandible shape and climate persisted with the first pair of axes explaining 35% of covariation (Fig. 7C). They positively correlated to each other (r = 0.677, p < 0.002) with negative scores being occupied by the polar bear that is extremely adapted to cold condition (lower annual temperatures, highly seasonal) while on the positive score the Tibetan bear occupied warmer areas. The angle vector between PLS1 shape of non-hibernating and *Ursus* taxa was 61 degree, high but still significantly different from 90 degrees (p < 0.0001) supporting a relatively parallel mechanism of shape/climate covariation between the two groups. The PLS analysis performed on *U. arctos* specimens only yielded non-significant pattern of shape covariation with climate although the correlation coefficient for the first pair of vectors was relatively high (r = 0.599, p = 0.25).

Variation Partition

Using the whole sample of 66 bear specimens with sex and geographic localities, taxonomy (in this analysis species categorisation) clearly represented the factor that explained most of shape variation in all cases (both alone as "Pure" component and in interaction with the

others, Fig. 8A, Table 5). There was a high degree of interaction between taxonomy and

climate (10%) while both size and sex explained a much smaller percentage in isolation (2

and 1% respectively). In this set of data all factors contributed significantly to shape variance

except sex when in isolation (Table 5).

Similar results occurred when the subset of *Ursus* species was analysed (N = 52, Fig 8B,

Table 5). In this subsample, size as pure component explained more than sex and climate (6%

vs 2.3% and <1% respectively) while strong interaction between taxonomy and climate was

confirmed again (9%) (Table 5). In this dataset climate is not a significant factor when in

siolation (Table 5). The nested subset of *Ursus arctos* reduced the sample to 36 specimens. A

different pattern emerged especially in the significance of the factors as pure components

(Fig. 8C, Table 5). Taxonomy and climate were all non-significant in isolation while both

size and sex explained respectively 7% and 6% of variance (Table 5).

Discussion

The mandibular morphology of bears distinguishes extant species with a high degree of

accuracy and both size and shape data are useful taxonomic characters. Previous research

mostly focused on the functional link between these traits and diet (Figueiridoet al. 2009;

Meloro 2011; van Heteren et al. 2016), even if strong taxonomic signal always emerged in

these datasets. Relative Warp and Discriminant function analyses (Fig. 2A, B) support the

high morphological divergence of giant panda extensively related to its specialised bamboo

feeding pattern and strong bite force (Christiansen 2007). Also the other tropical taxa (*M.*

ursinus, *H. malayanus*, *T. ornatus*) are quite distinctive and most of the morphological

overlap occurs only between specimens of the genus *Ursus*. Van Heteren et al. (2016)

identified similar degree of taxonomic separation using 3D landmarking and our DFA

classification results suggest that at least the mandibular morphology does not support any similarity between the genus *Melursus* and *Ursus.* Krause et al. (2008) proposed to merge both genera based on molecular evidence although Pagès et al. (2008) pointed out that the two should be separated based also on behavioural and physiological characters (e.g. the ability to hibernate). Our mandible data support separation between the two genera and also fail to identify any possible convergence between *Melursus* and *Tremarctos* previously proposed by Kitchener (2010). The sloth bear is well characterised by a high degree of insectivory, a feeding habit exhibited only during certain seasons by more omnivorous American black bears and brown bears. This explains *M. ursinus* unique mandibular shape that presents an enlarged premolar region and a reduced ramus area for the attachment of the masticatory muscles, thus resulting in ability to produce low bite force (Sacco and Van Valkenburgh 2004; Christiansen 2007). *Tremarctos* has been equally interpreted as a more herbivorous bear and in our RW and DF analyses it occupies morphospace region completely opposite to *Melursus*. Its smaller mandibular size equally allows discriminating this taxon from *Ursus* taxa.

Our nested approach evidences more subtle distinction among members of the genus *Ursus* with taxa like the polar bear, the Apennine bear and the Isabelline bear always emerging as statistically distinguishable in size and shape. Discriminant function analyses support this assertion due to the very high degree of classification accuracy recorded for these taxa and for the Tibetan bear (*U. thibetanus*, Table 3). Slater et al. (2010) already highlighted the specialised morphological adaptation of polar bear in relation to its rapid evolution and carnivorous feeding habit. This does not correspond to a mandible capable of producing relatively high bite force as in other specialised predatory carnivores (Christiansen 2007), but we note a more slender profile indicative of soft food consumption being this species a

specialised hunter of marine mammals, characterised by high percentage of fat in their body

tissues (Sterling and Archibald 1977; van Heteren et al. 2016).

A unique mandibular morphology occurs also in *U. thibetanus* when climatic

adaptations are concerned (Fig. 7C). Distinctive traits include a thick mandibular corpus, a

relatively short premolar region and a wide ramus. Scanty dietary studies support omnivory

for the Asiatic black bear with seasonal prevalence of vegetation (soft mast especially, Reid

et al. 1991; Hwang et al. 2002). Our limited sample does not allow obtaining more insights

about functional adaptation and ecogeographical variation in this species. Amano et al.

(2004) reported significant differences in skull morphologies of two Japanese populations of

U. thibetanus and a pattern of geographical changes occur also in our sample (Fig. 7C). This

remains to be explored more in detail especially in relation to other potential geographically

overlapped competitors such as the brown bear.

The subspecies *U. a. marsicanus* and *U. a. isabellinus* are a special case in point and

our data analyses are the first to support their uniqueness within a broad taxonomic context.

Indeed, they are the few amongst recognisable brown bear subspecies to not overlap with the

American black bear, and DFA record quite high percent of accuracy for these subspecies.

Adaptation to peculiar climatic condition does not provide a valuable explanation for their

distinctiveness due to the lack of a strongly significant association in brown bear between

mandible shape and climate (Fig. 7B, C and Table 5). Deformation grids from RW and DFA

(Figs. 4 and 5) describe consistently for the Apennine bear a mandible with very thick corpus

below the canine region, a relatively long diastema, a wide long and thick molar crushing

area. These shape features can be functionally associated with the high consumption of hard

mast by Apennine bears (Ciucci et al. 2014), and are also supported by parallel studies on its

cranial morphometry that highlighted changes in regions of masticatory muscles (Loy et al.

2008; Colangelo et al. 2012). For the Isabelline bear, earliest description by Pocock (1932,

1941) were validated by molecular data (Galbreath et al. 2007) that support a long

geographical isolation for this subspecies. Opposite to the Apennine bear, the mandible of

Isabelline bear is slender under the canine region although retains thick corpus in the

posterior crushing area. Aryal et al. (2012) described the diet of Isabelline brown bear on the

Nepalese mountain as prevailed by Alpine marmots. It might be likely that slender corpus

under canine region is an adaptation to hunt burrowing mammals, although a broader

taxonomic comparison with taxa of similar diet is required to list this trait as especially

adaptive for carnivorans of the Himalayan plateau.

A significant degree of mandibular morphological distinctiveness is recorded for *U. a.*

arctos and *U. a. dalli*, while specimens of *U. a. alascensis* can be correctly classified only

with a 50% of accuracy (Table 3). Molecular work from Waits et al. (1998) and Korsten et al.

(2009) on North American brown bear provides no substantial support for most of the

Alaskan subspecies characterisation, although significant genetic differences occur between

European and Alaskan brown bears. Our sample suggests that a degree of morphological

overlap might occur between North American and European brown bear subspecies as well

as the American black bear due to potentially similar climatic adaptations and plastic feeding

behaviour.

The Partial Least Square analysis supports climate to play a significant role in the

diversification of bears (Fig. 7) Mandibular shape profiles always show the corpus region to

evolve shorter and thicker in bears that occupy regions with relatively higher precipitation

(bio12, 16 and 18) while slender mandibular profiles characterise species from highly

seasonal environments (bio4 and 7). This happens in all cases (Figs. 7A, B, C) and explains

the lack of a significant difference in the relatively large (60 degrees) angle vector between

Ursus taxa (Fig. 7C) and the other non-hibernating species (Fig. 7B). Higher precipitations

might relate to higher availability of food and a broader dietary niche, hence thicker

mandibular corpus to deal with a variety of food. When *Ursus* taxa are analysed separately

the climatic patterns is driven by adaptation to dry extreme condition as seen along the

species gradient that goes from *U. maritimus* to *U. thibetanus*. Krause et al. (2008) described

the modern bear radiation as a rapid event that occurred during the Mio-Pliocene boundary, a

period characterised by drought and opening of savannah grassland ecosystem. Our data

suggest climate to have significant influence on species differentiation of modern bears

although this applies only to macroevolutionary scale. Indeed, variation partition shows

climate to have a non-significant influence when in isolation on the mandibular shape

differences of *Ursus* taxa and brown bear subspecies (Table 5). Sexual dimorphism instead

increase in relative importance at narrow taxonomic scale. Especially for *Ursus arctos* this

factor explains in isolation almost the same portion of variance as size while for *Ursus* spp. it

is almost 2%. Previous studies have reported sexual dimorphism in skulls of brown bear

(Ohdachi et al. 1992; Yoneda et al. 1976), polar bear (Bechshøft et al. 2008) and black bear

(Gordon Morejohn 1975) however its degree of interaction with taxonomy and climatic

variation was never reported before. Our analyses suggest that sexual dimorphism interact

quite significantly at all levels with mandibular size but not so much with taxonomy and

climate. Taxonomy on the other side, always explain a very high proportion of mandibular

shape variance in bear. To what extent then phylogenetic relatedness is reflected in bear

mandibular morphology? Considering our UPGMA and K_{multiv} approach phylogenetic signal

of bear mandibular shape data compare well with that observed in other mammalian groups

including Carnivora and Primates as whole where K_{multiv} was similarly around $0.5 - 0.6$

(Meloro et al. 2015b, c). Although mandible shape in Ursidae clearly reflects feeding

adaptations as evidenced by previous studies (Meloro 2011; van Heteren et al. 2016) we

support its relevance to detect subtle differences between species and subspecies at all levels.

More work is needed to clarify bear taxonomy, but our analyses strongly support the validity

of Apennine and Isabelline brown bear subspecies thus challenging future conservation

efforts.

Acknowledgments

References

Adams DC, Rohlf FJ, Slice DE (2004) Geometric morphometrics: ten years of progress

following the 'revolution'. Ital J Zool **71:**5−16.

Adams DC, Otárola-Castillo E (2013) Geomorph: an R package for the collection and

analysis of geometric morphometric shape data. Meth Ecol Evol **4:**393−399.

Adams DC, Rohlf FJ, Slice DE (2013) A Field Comes of Age: Geometric Morphometrics in

the 21st Century. Hystrix, Ital J Mammal **24:**7−14.

Adams DC (2014) A generalized K statistic for estimating phylogenetic signal from shape

and other high-dimensional multivariate data. Syst Biol **63:**685−697.

Adams DC, Collyer ML (2015) Permutation tests for phylogenetic comparative analyses of

high-dimensional shape data: What you shuffle matters. Evolution **69:**823−829.

Amano M, Oi T, Hayano A (2004) Morphological differentiation between adjacent populations of Asiatic black bears, *Ursus thibetanus japonicus*, in northern Japan. J Mammal **85:**311−315.

Arnold C, Matthews LJ, Nunn CL (2010) The 10k Trees website: a new online resource for primate phylogeny. Evol Anthropol **19:**114–118.

Aryal A, Hopkins III JB, Raubenheimer D, Ji W, Brunton D (2012) Distribution and diet of brown bears in the upper Mustang Region, Nepal. Ursus **23:**231−236.

Baryshnikov GF, Mano T, Masuda R (2004) Taxonomic differentiation of *Ursus arctos* (Carnivora, Ursidae) from south Okhotsk Sea islands on the basis of morphometrical analysis of skull and teeth. Russ J Theriol **3:**77−88.

Banes GL, Galdikas BM, Vigilant L (2016) Reintroduction of confiscated and displaced mammals risks outbreeding and introgression in natural populations, as evidenced by orang-utans of divergent subspecies. Sci Rep **6:**22026.

Barnes I, Matheus P, Shapiro B, Jensen D, Cooper A (2002) Dynamics of Pleistocene Population Extinctions in Beringian Brown Bears. Science **295:**2267−2270.

Blomberg SP, Garland T, Ives AR (2003) Testing for phylogenetic signal in comparative data: behavioral traits are more labile. Evolution **57:**717−745.

Bojarska K, Selva N (2012) Spatial patterns in brown bear Ursus arctos diet: the role of geographical and environmental factors. Mamm Rev **42:**120−143.

Bechshøft TØ, Sonne C, Rigét FF, Wiig Ø, Dietz R. (2008) Differences in growth, size and sexual dimorphism in skulls of East Greenland and Svalbard polar bears (*Ursus maritimus*). Polar Biology **31**: 945−958.

Bookstein FL. 1989. Principal warps: thin-plate splines and the decomposition of deformations. IEE, Trans Patt Anal Mach Intell **11:**567–585.

Bubadué JM, Cáceres N, Carvalho RS, Meloro C (2016) Ecogeographical Variation in Skull

Shape of South-American Canids: Abiotic or Biotic Processes? Evol Biol **43:**145−159.

Byun S, Koop BF, Reimchen TE (1997) North American black bear mtDNA

phylogeography: implications for morphology and the Haida Gwaii glacial refugium

controversy. Evolution **51:**1647−1653.

Cáceres N, Meloro C, Carotenuto F, Passaro F, Sponchiado J, Melo GL, Raia P (2014)

Ecogeographical variation in skull shape of capuchin monkeys. J Biogeogr **41:**501−512.

Cáceres NC, Weber MM, Melo GL, Meloro C, Sponchiado J, Carvalho RS, Bubadué JM

(2016) Which factors determine spatial segregation in the south American opossums

(*Didelphis aurita* and *D. albiventris*)? An ecological niche modelling and geometric

morphometrics approach. PloS one **11**: e0157723.Calvignac S, Hughes S, Tougard C,

Michaux J, Thevenot M, Philippe M, Hamdine W, Hänni C (2008) Ancient DNA evidence

for the loss of a highly divergent brown bear clade during historical times. Mol

Ecol **17:**1962−1970.

Cardini A, Jansson AU, Elton S (2007) A geometric morphometric approach to the study of

ecogeographical and clinal variation in vervet monkeys. J Biogeogr **34:**1663–1678.

Cardini A, Elton S (2008) Does the skull carry a phylogenetic signal? Evolution and

modularity in the guenons. Biol J Linn Soc **93:**813−834.

Cardini A (2014) Missing the third dimension in geometric morphometrics: how to assess if

2D images really are a good proxy for 3D structures? Hystrix, Ital J Mammal **25:**73−81.

Christiansen P (2007) Evolutionary implications of bite mechanics and feeding ecology in

bears. J Zool **272:**423−443.

Ciucci P, Tosoni E, Di Domenico G, Quattrociocchi, F, Boitani L (2014) Seasonal and annual

variation in the food habits of Apennine brown bears, central Italy. J Mammal **95:**572−586.

Colangelo P, Loy A, Huber D, Gomerĉić T, Vgna Taglianti A, Ciucci P (2012) Cranial

distinctiveness in the Apennine brown bear: genetic drift effect or ecophenotypic adaptation?

Biol J Linn Soc **107:**15−26.

Cronin MA (1993) In my experience: mitochondrial DNA in wildlife taxonomy and

conservation biology: cautionary notes. Wildlife Soc B (1973-2006) **21:**339−348.

Ewer RF (1973) The Carnivores. New York: Cornell University Press.

Figueirido B, Palmqvist P, Pérez-Claros JA (2009) Ecomorphological correlates of

craniodental variation in bears and paleobiological implications for extinct taxa: an approach

based on geometric morphometrics. J Zool **277:**70−80.

Fuchs M, Geiger M, Stange M, Sánchez-Villagra MR (2015) Growth trajectories in the cave

bear and its extant relatives: an examination of ontogenetic patterns in phylogeny. BMC Evol

Biol **15:**239.

Galbreath GJ, Groves CP, Waits LP (2007) Genetic resolution of composition and

phylogenetic placement of the isabelline bear. Ursus **18:**129−131.

Garshelis, DL, Crider D, van Manen F. (IUCN SSC Bear Specialist Group) (2008) Ursus

americanus. The IUCN Red List of Threatened Species 2008**:**e.T41687A10513074.

http://dx.doi.org/10.2305/IUCN.UK.2008.RLTS.T41687A10513074.en. Downloaded on 01

October 2016.

Gittleman JL (1985) Carnivore body size: ecological and taxonomic correlates. Oecol

67:540–554.

Gordon KR, Morejohn GV (1975) Sexing black bear skulls using lower canine and lower

molar measurements. J Wildl Managet 40-44.

Hall ER (1981) The mammals of North America (Vol. 2). New York: John Wiley, 2nd edn.

Herrero S (1999) Chapter 1: Introduction. In: Servheen C, Herrero S, Peyton B, Pelletier K, Moll K, Moll J (eds) Bears: status survey and conservation action plan (Vol. 44). IUCN, pp 1−7.

Hijmans, RJ, Cameron, SE, Parra, JL, Jones, PG, Jarvis, A (2005) Very high resolution interpolated climate surfaces for global land areas. International Journal of Climatology **25:**1965−1978.

Hwang MH, Garshelis DL, Wang Y (2002) Diets of Asiatic black bears in Taiwan, with methodological and geographical comparisons. Ursus **13:**111−125.

IUCN (2016) The IUCN Red List of Threatened Species. Version 20162. <http://www.iucnredlist.org>. Downloaded on 04 October 2016

Kennedy ML, Kennedy PK, Bogan MA, Waits JL (2002) Geographic variation in the black bear (*Ursus americanus*) in the eastern United States and Canada. Southwest Nat **47:**257−266.

Kitchener AC (2010) Taxonomic issues in bears: impacts on conservation in zoos and the wild, and gaps in current knowledge. International Zoo Yearbook **44:**33−46.

Korsten M, Ho SY, Davison J, Pähn B, Vulla E, Roht M, Tumanov IL, Kojola I, Andersone-Lilley Z, Ozolins J, Pilot M, Mertzanis Y, Giannakopoulus A, Vorobiev AA, Markov NI, Saveljev AP, Lyapunova EA, Abramov AV, Männil P, Valdmann H, Pazetnov SV, Pazetnov VS, Rõkov AM, Saarma U (2009) Sudden expansion of a single brown bear maternal lineage across northern continental Eurasia after the last ice age: a general demographic model for mammals? Mol Ecol **18:**1963−1979.

Krause J, Unger T, Noçon A, Malaspinas AS, Kolokotronis SO, Stiller M, Soibelzon L, Spriggs H, Dear PH, Briggs AW, Bray SCE, O'Brien SJ, Rabeder G, Matheus P, Cooper A, Slatkin M, Pääbo S, Hofreiter M (2008) Mitochondrial genomes reveal an explosive radiation of extinct and extant bears near the Miocene-Pliocene boundary. BMC Evol Biol **8:**220.

Loy A, Genov P, Galfo M, Jacobone MG, Vigna Taglianti A (2008) Cranial morphometrics of the Apennine brown bear (*Ursus arctos marsicanus*) and preliminary notes on the relationships with other southern European populations. Ital J Zool **75:**67−75.

Mattson DJ (1998) Diet and morphology of extant and recently extinct northern bears. Ursus **10:**479−496.

McLellan, B.N., Servheen, C. & Huber, D. (IUCN SSC Bear Specialist Group) (2008) *Ursus arctos*. The IUCN Red List of Threatened Species 2008: e.T41688A10513490. http://dx.doi.org/10.2305/IUCN.UK.2008.RLTS.T41688A10513490.en. Downloaded on 04 October 2016.

Meijaard E (2004) Craniometric differences among Malayan sun bears (Ursus malayanus); evolutionary and taxonomic implications. Raffles B Zool **52:**665−672.

Meloro C (2011) Feeding habits of Plio-Pleistocene large carnivores as revealed by the mandibular geometry. J Vert Paleontol **31:**428−446.

Meloro C, O'Higgins P (2011) Ecological adaptations of mandibular form in fissiped Carnivora. J Mamm Evol **18:**185−200.

Meloro C (2012) Mandibular shape correlates of tooth fracture in extant Carnivora: implications to inferring feeding behaviour of Pleistocene predators. Biol J Linn Soc **106:**70−80.

Meloro C, Elton S, Louys J, Bishop LC, Ditchfield P (2013) Cats in the forest: predicting habitat adaptations from humerus morphometry in extant and fossil Felidae (Carnivora). Paleobiology **39:**323−344.

Meloro C, Cáceres N, Carotenuto F, Sponchiado J, Melo GL, Passaro F, Raia P (2014a) In and out the Amazonia: evolutionary ecomorphology in howler and capuchin monkeys. Evol Biol **41:**38−51.

Meloro C, Cáceres N, Carotenuto F, Passaro F, Sponchiado J, Melo GL, Raia P (2014b)
Ecogeographical variation in skull morphometry of howler monkeys (Primates: Atelidae).
Zool Anz **253:**345−359.

Meloro C, Hudson A, Rook L (2015a) Feeding habits of extant and fossil canids as
determined by their skull geometry. J Zool **295:**178−188.

Meloro C, Clauss M, Raia P (2015b) Ecomorphology of Carnivora challenges convergent
evolution. Org Div & Evol 15:711−720.

Meloro C, Cáceres NC, Carotenuto F, Sponchiado J, Melo GL, Passaro F, Raia P (2015c)
Chewing on the trees: Constraints and adaptation in the evolution of the primate mandible.
Evolution **69:**1690−1700.

Mihaylov R, Dimitrov R, Raichev E, Kostov D, Stamatova-Yiovcheva K, Zlatanova D,
Bivolarski B (2013) Morphometrical features of the head skeleton in Brown Bear (*Ursus
arctos*) in Bulgaria. Bulg J Agric Sci **19:**331−337.

Oksanen J, Blanchet FG, Kindt R, Legendre P, Minchin PR, O'Hara RB, Simpson GL,
Solymos P, Stevens MHH, Wagner H (2012) R Package Version 2.0-4. Community Ecology
Package, Vegan.

Ohdachi S, Toshiki AOI, Tsubota T (1992) Growth, sexual dimorphism, and geographical
variation of skull dimensions of the brown bear *Ursus arctos* in Hokkaido. J Mamm Soc Jap
17: 27–47.

Pagès M, Calvignac S, Klein C, Paris M, Hughes S, Hänni C (2008) Combined analysis of
fourteen nuclear genes refines the Ursidae phylogeny. Mol Phylogenet Evol **47:**73−83.

Pocock RI (1932) The black and brown bears of Europe and Asia. Part II. J Bomb Nat Hist
Soc **36:**1101–138.

Pocock RI (1941) The fauna of British India, including Ceylon and Burma. Mammalia. Volume II. Carnivora (continued from Volume I), Suborders Aeluroidea (part) and Arctoidea. London, UK: Taylor and Francis.

Rausch RL (1963) Geographic variation in size in North American brown bears, Ursus arctos L., as indicated by condylobasal length. Can J Zool **41:**33−45.

Reid D, Jiang M, Teng Q, Qin Z, Hu J (1991) Ecology of the Asiatic black bear (Ursus thibetanus) in Sichuan, China. Mammalia **55:**221–238.

Rohlf FJ (2000) Statistical power comparisons among alternative morphometric methods. Am J Phys Anthropol **111:**463−478.

Rohlf FJ (2015) The tps series of software. Hystrix, It J Mammal **26:**1−4.

Rohlf FJ, Slice D (1990) Extensions of the Procrustes method for the optimal superimposition of landmarks. Syst Biol **39:**40−59.

Rohlf FJ, Corti M (2000) Use of two-block partial least-squares to study covariation in shape. Syst Biol **49:**740–753.

Sacco T, Van Valkenburgh B (2004) Ecomorphological indicators of feeding behaviour in the bears (Carnivora: Ursidae). J Zool **263:**41−54.

Slater GJ, Figueirido B, Louis L, Yang P, Van Valkenburgh B (2010) Biomechanical consequences of rapid evolution in the polar bear lineage. PloS One **5:**e13870.

van Heteren AH, MacLarnon A, Rae TC, Soligo C (2009) Cave bears and their closest living relatives: a 3D geometric morphometrical approach to the functional morphology of the cave bear Ursus spelaeus. Acta carsologica **47:**33−46.

van Heteren AH, MacLarnon A, Soligo C, Rae TC (2014) Functional morphology of the cave bear (Ursus spelaeus) cranium: a three-dimensional geometric morphometric analysis. Quat Intern **339:**209−216.

van Heteren AH, MacLarnon A, Soligo C, Rae TC (2016) Functional morphology of the cave

bear (Ursus spelaeus) mandible: a 3D geometric morphometric analysis. Org Div & Evol

16:299−314.

Yoneda M, Abe H (1976) Sexual dimorphism and geographic variation in the skull of the Ezo

Brown Bear (*Ursus arctos yesoensis*). Memoirs of the Faculty of Agriculture-Hokkaido

University (Japan).

Waits LP, Talbot SL, Ward RH, Shields GF (1998) Mitochondrial DNA phylogeography of

the North American brown bear and implications for conservation. Conserv Biol

12:408−417.

Waits LP, Sullivan J, O'Brien SJ, Ward RH (1999) Rapid Radiation Events in the Family

Ursidae Indicated by Likelihood Phylogenetic Estimation from Multiple Fragments of

mtDNA. Mol Phyl Evol **13:**82−92.

Wilson DE, Reeder DM (2005) Mammal species of the world: a taxonomic and geographic

reference (Vol. 1). JHU Press, 3rd edn.

Zedrosser A, Dahale B, Swenson JE, Gerstl N (2001) Status and management of the brown

bear in Europe. Ursus **12:**9−20.

Zelditch ML, Swiderski DL, Sheets HD, Fink WL (2004) Geometric morphometrics for

biologists: A primer. London: Elsevier Academic Press.

Figure Legends

Fig. 1. Landmark configuration on a mandibular outline of brown bear (*Ursus arctos*).

Landmark definitions are as follow: 1 anterior tip of canine alveolus; 2 posterior tip of the

canine alveolus; 3 anterior tip of alveolar premolar 4 (p4) edge; 5 anterior tip of the alveolar

lower carnassial (m1) edge; 6 lower alveolar edge defining m1 slicing area; 7 posterior edge

of m3 alveolus; 7 most superior tip of the coronoid process; 8 and 9 anterior and posterior

tips of mandibular condyle in lateral view; 10 posterior tip of the angular process; 11 ventral

extreme of the angular process; 12, 13 and 14 are projection of landmarks 2, 4 and 12

perpendicular to the line 1-6

Fig. 2. Scatterplot of: (a) the first two Relative Warp axes obtained from shape variables.

Deformation grids at the onset of each axes show relative shape changes from the mean

described by each RW vector, (b) the first three Discriminant Function vectors obtained from

a combination of shape coordinates and size. Deformation grids at the onset of each DF axes

were obtained by regressing original shape coordinates vs DF vector scores. Label colours

according to species

Fig. 3. Mandible shape deformation related to size from the smallest (*H. malayanus*) to the largest (*U. arctos*) bear species with a box plot showing differences in natural log transformed centroid size ursid species

Fig. 4. Scatterplot of: (a) the first two Relative Warp axes obtained from shape variables. Deformation grids at the onset of each axes show relative shape changes from the mean described by each RW vector; (b) the first two Discriminant Function vectors obtained from a combination of shape coordinates and size. Deformation grids at the onset of each DF axes were obtained by regressing original shape coordinates vs DF vector scores. Label colours according to *Ursus* species and subspecies of *U. arctos*

Fig. 5. Scatterplot of: (a) the first two Relative Warp axes obtained from shape variables. Deformation grids at the onset of each axes show relative shape changes from the mean described by each RW vector: (b) the first two Discriminant Function vectors obtained from a combination of shape coordinates and size. Deformation grids at the onset of each DF axes were obtained by regressing original shape coordinates vs DF vector scores. Label colours according to subspecies of *U. arctos*

Fig. 6. Phylogenetic hypothesis for extant bears based on molecular data (a) followed by UPGMA trees of Procrustes distances from mandible shape data inclusive of: (b) all eight species of bears, (c) *Ursus* species and *U. arctos* subspecies, and (d) *U. arctos* subspecies only

Fig. 7. Scatterplot of the first pair of Partial Least Squares vectors for: (a) all Ursidae; (b) all tropical ursid species; (c) all *Ursus* spp. Variable and shape vectors are given respectively along the ordinate and the abscissa. Deformation grids show shape changes in correspondence of the extremes the first axis while variables profiles give the estimate of the standardized scores of each variable as vertical lines extending from a horizontal axis corresponding to the mean

Fig. 8. Schematic depiction of the factors size, sex, taxonomy and climate included in variation partition analysis meant to illustrate their individual contribution and relative interaction to mandible shape variance. We used a sample of mandibles with geographic locations of (a) all Ursidae (N = 66); (b) all *Ursus* spp. (N = 52); (c) all *U. arctos* (N = 36)

Tables

Table 1. Procrustes ANOVA and ANOVA to test the impact of taxonomy and sex (and their interaction) on mandible shape and size for 74 sexed Ursidae specimens. Significance is highlighted in bold

		df	SS	MS	R²	F	p
	Species	7	0.16145	0.02306	0.50046	9.6123	**1.00E-04**
SHAPE	Sex	1	0.00895	0.00895	0.02775	3.7303	**0.0002**
	Species x Sex	6	0.01063	0.00177	0.03296	0.7386	0.7614
	Residuals	59	0.14157	0.0024			
	Total	73	0.32261				
	Species	7	2.0961	0.29945	0.54942	14.1578	**1.00E-04**
SIZE	Sex	1	0.4021	0.40205	0.10538	19.0091	**0.0002**
	Species x Sex	6	0.0691	0.01152	0.01811	0.5445	0.7213
	Residuals	59	1.2479	0.02115			
	Total	73	3.8152				

Table 2. Procrustes ANOVA and ANOVA to test the impact of taxonomy and sex (and their interaction) on mandible shape and size for 53 sexed *Ursus* spp. specimens. In this analysis brown bear taxonomy is subdivided into subspecies. Significance is highlighted in bold

		df	SS	MS	R²	F	p
SHAPE	Species	8	0.057256	0.007157	0.37884	3.6923	**1.00E-04**
	Sex	1	0.008089	0.0080893	0.05352	4.1733	**0.0002**
	Species x Sex	8	0.017948	0.0022435	0.11875	1.1574	**0.0261**
	Residuals	35	0.067842	0.0019383			
	Total	52	0.151135				
SIZE	Species	8	1.29453	0.161817	0.64402	19.7597	**1.00E-04**
	Sex	1	0.30872	0.308722	0.15359	37.6987	**1.00E-04**
	Species x Sex	8	0.1202	0.015025	0.0598	1.8347	**0.0441**
	Residuals	35	0.28662	0.008189			
	Total	52	2.01008				

Table 3. Percentage of correctly classified cases obtained for *Ursus* taxa after cross validation using discriminant function analysis. In the first column results are shown for the DFA extracted analysing *Ursus* taxa only (N = 119) while on the second the dataset was reduced for *U. arctos* subspecies only (N = 78)

	Ursus %	*U.arctos* %
U. a. alascensis	50	50
U. a. arctos	67.9	67.9
U. a. dalli	66.7	66.7
U. a. horribilis	50	60
U. a. isabellinus	71.4	85.7
U. a. marsicanus	94.1	100
U. americanus	62.5	
U. maritimus	90.9	
U. thibetanus	85.7	

Table 4. Procrustes ANOVA and ANOVA to test the impact of taxonomy and sex (and their interaction) on mandible shape and size for 37 sexed *Ursus arctos*. specimens. In these

analyses brown bear taxonomy is subdivided into subspecies. Significance is highlighted in bold

		df	SS	MS	R²	F	p
	Species	5	0.031452	0.0062905	0.33298	3.3837	**1.00E-04**
SHAPE	Sex	1	0.005168	0.0051681	0.05471	2.78	**0.0033**
	Species x Sex	5	0.011361	0.0022722	0.12028	1.2222	**0.0428**
	Residuals	25	0.046477	0.0018591			
	Total	36	0.094459				
	Species	5	0.65416	0.130832	0.59205	16.3032	**1.00E-04**
SIZE	Sex	1	0.1743	0.1743	0.15775	21.7199	**1.00E-04**
	Species x Sex	5	0.07583	0.015166	0.06863	1.8898	0.0731
	Residuals	25	0.20062	0.008025			
	Total	36	1.10491				

Table 5. Variation partition performed using different subsamples of mandibular shape data

as explained variables (Y). The exploratory variables include mandibular log transformed

centroid size (size), sex, species classification (taxonomy), and climate (simplified by 19

bioclimatic variables subjected to Principal Component Analysis-only the first five PCs

explaining >95% were included). Non significance is highlighted in bold

Sample	Exploratory variables	Df	R2	Adj.R2	F	P
Ursidae (N = 66)	[aeghklno] = X1 (Size)	1	0.06731	0.05273	4.6184	0.001
	[befiklmo] = X2 (Sex)	1	0.04692	0.03203	3.1508	0.002
	[cfgjlmno] = X3 (Taxonomy)	7	0.47608	0.41285	7.5293	0.001
	[dhijkmno] = X4 (Climate)	5	0.22709	0.16268	2.9893	0.001
	Individual fractions					
	[a] = X1 | X2+X3+X4	1		0.01984	2.8318	0.008
	[b] = X2 | X1+X3+X4	1		0.00777	1.8539	**0.065**
	[c] = X3 | X1+X2+X4	7		0.26785	4.9779	0.001
	[d] = X4 | X1+X2+X3	5		0.02111	1.3804	0.046
Ursus (N = 52)	[aeghklno] = X1 (Size)	1	0.07224	0.05369	3.8933	0.001
	[befiklmo] = X2 (Sex)	1	0.06922	0.0506	3.7182	0.001
	[cfgjlmno] = X3 (Taxonomy)	9	0.39037	0.25973	2.9882	0.001
	[dhijkmno] = X4 (Climate)	5	0.21137	0.12565	2.4658	0.001
	Individual fractions					
	[a] = X1 | X2+X3+X4	1		0.05989	4.4282	0.001
	[b] = X2 | X1+X3+X4	1		0.02278	2.3039	0.015
	[c] = X3 | X1+X2+X4	9		0.16856	2.0006	0.001
	[d] = X4 | X1+X2+X3	5		0.00826	1.105	**0.293**
U. arctos (N = 36)	[aeghklno] = X1 (Size)	1	0.0892	0.06241	3.3299	0.005
	[befiklmo] = X2 (Sex)	1	0.05939	0.03173	2.1468	0.039
	[cfgjlmno] = X3 (Taxonomy)	6	0.35707	0.22404	2.6843	0.001
	[dhijkmno] = X4 (Climate)	5	0.25644	0.13251	2.0693	0.003
	Individual fractions					
	[a] = X1 | X2+X3+X4	1		0.06594	2.1696	0.002
	[b] = X2 | X1+X3+X4	1		0.06464	3.2885	0.005
	[c] = X3 | X1+X2+X4	6		0.1628	1.0144	**0.454**
	[d] = X4 | X1+X2+X3	5		0.00173	1.0144	**0.449**

Appendix 1. List of analysed bear specimens with geographic location.

Acronyms:
Sex - M = Male, F = Female, U = unknown
Museums abbreviation

NHM	Natural history museum of London
AMNH	American Museum of Natural History
PANLM	Parco Nazionale d'Abruzzo Lazio & Molise
NMNHS	National Museum of Natural History, Sofia, Bulgaria
MC	Museo di Anatomia Comparata, Roma
La Specola	Museo di Storia Naturale La Specola
ZMCU	Zoological Museum, University of Copenhagen
WML	World Museum Liverpool

Species	Sex	Museum	Catalogue #	Locality	Lat	Long
U.arctos	M	NHM	53.568	Unknown		
U.arctos	U	LaSpecola	C11883	Unknown		
U.a.horribilis	F	NHM	18.4.6.1	Montana, USA	46.87968	-110.363
U.a.marsicanus	U	LaSpecola	C3584	Unknown	41.86956	13.7068
U.thibetanus	U	NHM	219b	Nepal	28.5287	83.5111
U.thibetanus	U	MC	6669	Unknown		
U.americanus	U	NHM	1938.11.28.1	Unknown		
U.americanus	U	NHM	43.11.28.5	Albany District, Canada	52.025	-81.616
U.americanus	U	MC	444	Unknown		
U.americanus	F	NHM	61.1282	Alaska, USA	64.20084	-149.494
H.malayanus	M	NHM	1938.11.30.70	Sumatra	0.3515	100.4699
H.malayanus	U	HM	V5648	Unknown		
H.malayanus	U	HM	No Cat	Unknown		
H.malayanus	U	MC	7951	Unknown		
M.ursinus	F	NHM	34.8.12.9	Roul, India	10.5655	77.4794
M.ursinus	M	NHM	35.1.1.5	Kollegal, India	12.15	77.1167
M.ursinus	F	NHM	25.5.22.1	Sal jungle, Bankhura Bengal, India	23.2371	87.0652
M.ursinus	U	NHM	34.10.18.4	Surgara State CP India, Mabaraj Kanar of Bikaner, India	28.0167	73.3118
M.ursinus	U	NHM	88.3.20.1.220	Madras, India	13.0524	80.2508
M.ursinus	U	NHM	24.10.5.9	Singhbhum Chota Nagpur, India	23.2139	83.2228
T.ornatus	U	NHM	3.6.27.5	Conipiten Tsumbari, Peru	-7.8125	-76.3864
T.ornatus	M	NHM	36.9.2.70	Inchachaca, Bolivia	-16.4167	-68.0667

Species	Sex	Coll	Catalog No.	Locality	Latitude	Longitude
T.ornatus	M	NHM	27.11.1.71	Peru	-7.8125	-76.3864
T.ornatus	F	NHM	9.7.26.1	Merida, Venezuela	8.6	-71.15
A.melanoleuca	U	NHM	1938.71	Unknown	31.5625	104.875
A.melanoleuca	M	NHM	39.3808	Berejowsky, China	31.5625	104.875
A.melanoleuca	U	NHM	55.587	Unknown	31.5625	104.875
A.melanoleuca	U	NHM	1938.55.590	Szechwan, China	30.65165	104.0759
A.melanoleuca	U	NHM	1938.55.591	Szechwan, China	30.65165	104.0759
A.melanoleuca	U	NHM	1938.55.588	Szechwan, China	30.65165	104.0759
A.melanoleuca	U	NHM	96.8.20.1	Szechwan, China	30.65165	104.0759
A.melanoleuca	U	NHM	1938.55.589	Szechwan, China	30.65165	104.0759
A.melanoleuca	U	NHM	1938.55.592	Szechwan, China	30.65165	104.0759
T.ornatus	U	NHM	55.12.24.309	Unknown		
T.ornatus	U	NHM	1939.3617	Mountain Aminok (not found)		
T.ornatus	U	NHM	73.6.27.4b	Cosimpaba Immburi River, Peru	-7.8125	-76.3864
T.ornatus	M	NHM	70.369	Unknown		
T.ornatus	U	NHM	19664.4.13.2	Unknown		
T.ornatus	U	NHM	78.8.31.12	Ecuador	-1.8312	-78.1834
T.ornatus	U	NHM	81.784	Unknown		
M.ursinus	U	NHM	62.1062	South Chumda, China	32.9932	97.0088
M.ursinus	U	NHM	30.3.23.43	Unknown		
M.ursinus	U	NHM	220a	Unknown		
M.ursinus	U	NHM	31.1.10.9bc	Unknown		
M.ursinus	U	NHM	20.10.27.ab	Unknown		
M.ursinus	U	NHM	30.3.2.1	Gauripor, Assam, India	26.2006	92.9375
M.ursinus	M	NHM	20.10.27.5b	South Chumda, China	32.9932	97.0088
M.ursinus	F	NHM	36.1.22.2b	Pallanoum Ceylon, Sri Lanka	7.873054	80.7718
M.ursinus	U	NHM	24.10.5.11b	Singhbhum Chota Nagpur, India	23.2139	83.2228
U.americanus	F	NHM	61.1284b	Eagle Rvier near Anchorage, Alaska	61.21806	-149.9
U.americanus	U	NHM	1976.197	coll. Vanderby, Alaska	64.20084	-149.494
U.arctos	U	NHM	62.3.29.8b	Sweden, Mr Llouds Collection		
U.arctos	U	NHM	78.6.18.1	Stuffed specimen in Collect Namerica coll. Ward, Alaska, USA	63.0168	-157.478
U.arctos	F	NHM	87.12.22.1	Northern Steppe West End Caucasus 70°00'		

U.arctos	M	NHM	1010G	Zool. Soc. London Launrus-Dehra Dun-P 9000!		
U.thibetanus	M	NHM	26.10.8.41	NWP, India	30.3164	78.0321
U.thibetanus	M	NHM	22.12.22.5b	Okotso, Naga Hills, 3000 ft, Myanmar	26.4759	95.2727
U.thibetanus	U	NHM	91.11.21.1	Near Tonghoo, Myanmar	18.9333	96.4333
U.thibetanus	F	NHM	30.5.21.2	Vernagi Kashmir, India	33.5377	75.2449
U.thibetanus	M	NHM	31.9.21.4	TunJal PirPanjal 1500 ft Jrashuir, India	33.8602	74.3994
U.a.marsicanus	F	PNALM	164M	Unknown	41.86956	13.7068
U.a.marsicanus	F	PNALM	165M	Unknown	41.86956	13.7068
U.a.marsicanus	U	PNALM	167M	Lecce Vecchio, Italy	41.86956	13.7068
U.a.marsicanus	M	PNALM	174M	Ferro di Cavallo (Gioia dei Marsi-Lecce dei Marsi), Italy	41.95495	13.69446
U.a.marsicanus	F	PNALM	178M	Unknown	41.86956	13.7068
U.a.marsicanus	M	PNALM	179M	Paolura-Val Fondillo (Opi), Italy	41.78021	13.82969
U.a.marsicanus	F	PNALM	180M	Pietrascritta(Ortucchio), Italy	41.95883	13.64521
U.a.marsicanus	M	PNALM	184M	Difesa di Pescasseroli, Italy	41.80785	13.78879
U.a.marsicanus	M	PNALM	185M	Cantone di Villavallelonga, Italy	41.87157	13.62088
U.a.marsicanus	U	PNALM	186M	Monteo(Civitella Roveto), Italy	41.91365	13.42862
U.a.marsicanus	U	PNALM	187M	Metuccia, Italy	41.6833	13.9333
U.a.marsicanus	F	PNALM	258M	Colle Pizzuto (Civittela Alfedena), Italy	41.76536	13.94276
U.a.marsicanus	F	PNALM	259M	Villavallelonga, Italy	41.87157	13.62088
U.a.marsicanus	M	PNALM	260M	Terraegna (Pescasseroli), Italy	41.80785	13.78879
U.a.marsicanus	F	PNALM	262M	Val Fondillo (Opi), Italy	41.78021	13.82969
U.a.marsicanus	M	PNALM	696M	Zoo di Pescasseroli, Italy	41.80785	13.78879
U.maritimus	U	NHM	unreg	North Sea	79.812	23.686
U.maritimus	U	NHM	45.12.29.8	North Sea	79.812	23.686
U.maritimus	U	NHM	55.11.26.72	Wellington Channel, Barrow Strait, Cpt. Pullen	75.16667	-93

44

U.maritimus	U	NHM	1937.5.6.5	Kanderhogvak, Greenland	71.74643	-28.3887
U.maritimus	U	NHM	1937.11.3.1	Mygg Burta, Greenland	71.74643	-28.3887
U.maritimus	F	NHM	1938.11.11.8	Southampton (British Canadian Artic), Canada	64.599	-84.134
U.maritimus	U	MC	440	Unknown		
U.maritimus	M	NHM	90.8.4.1	Griffin Bay Wellington Channel (Polar Seas), Canada	75.16667	-93
U.a.arctos	U	NMNHS	10-16ML	Rila mountains, Bulgaria	42.1333	23.5499
U.a.arctos	U	NMNHS	11-17ML	Rila mountains, Bulgaria	42.1333	23.5499
U.a.arctos	U	NMNHS	13-2ML	Rila mountains, Bulgaria	42.1333	23.5499
U.a.arctos	U	NMNHS	2-2ML	Rila mountains, Bulgaria	42.1333	23.5499
U.a.arctos	U	NMNHS	5-15Ml	Rila mountains, Bulgaria	42.1333	23.5499
U.a.arctos	U	NMNHS	8-13ML	Rila mountains, Bulgaria	42.1333	23.5499
U.a.arctos	U	NMNHS	9-14ML	Rila mountains, Bulgaria	42.1333	23.5499
H.malayanus	M	AMNH	19155	Borneo	1.068	114.233
H.malayanus	U	AMNH	28254	Borneo	1.068	114.233
H.malayanus	F	AMNH	35364	Unknown		
H.malayanus	F	AMNH	35484	zoo NYC		
H.malayanus	U	AMNH	60772	Unknown		
H.malayanus	U	AMNH	89854	Unknown		
M.ursinus	F	AMNH	54464	Nepal	28.394	84.124
M.ursinus	F	AMNH	54465	Nepal	28.394	84.124
M.ursinus	U	AMNH	54466	Madhya Pradesh, Saharanpur North Kheriforest, India	29.967	77.551
M.ursinus	M	AMNH	54467	Saharanpur North Kheriforest, India	29.967	77.551
M.ursinus	F	AMNH	90388	Unknown		
U.arctos	M	AMNH	183132	Japan	39.469	140.903
U.arctos	M	AMNH	85407	Amurland,Nelta River,60mi N of Khabarovsk, Russia	48.712	134.989
U.a.dalli	F	AMNH	166746	Yakutat,Mouth of Russell fyord,West shore, Alaska, USA	59.554	-139.297
U.a.dalli	F	AMNH	66747	Yakutat,Don river flats, Alaska, USA	59.546	-139.727
U.a.dalli	M	AMNH	169530	Yakutat, Alaska, USA	59.546	-139.727

45

U.a.gyas	M	AMNH	135505	Kenai Peninsula,Canoe bay, Alaska, USA	64.20084	-149.494
U.a.horribilis	F	AMNH	129378	Yellow park, Wyoming, USA	44.513	-109.103
U.a.horribilis	M	AMNH	129379	Yellow park, Wyoming, USA	44.513	-109.103
U.a.horribilis	M	AMNH	167875	Spanish lake, Canada	47.301	-82.43
U.a.horribilis	U	WML	1963.173.38	Montana, USA	46.879	-110.362
U.a.horribilis	U	WML	1963.173.40	Utah, USA	39.32	-111.093
U.a.horribilis	M	AMNH	34403	Langton bay, Northwest Territories, Canada	69.417	-125.167
U.a.horribilis	F	AMNH	34404	Horton river, Northwest Territories, Canada	67.843	-120.75
U.a.horribilis	U	WML	7.3.78.1	Wyoming, USA	43.075	-107.29
U.a.isabellinus	U	WML	13.11.75.6	Kashmir, India	31.727	75.512
U.a.isabellinus	U	WML	13.11.75.7	Kashmir, India	31.727	75.512
U.a.isabellinus	U	WML	1963.173.35	Kashmir, India	31.727	75.512
U.a.isabellinus	U	WML	1963.173.36	Kashmir, India	31.727	75.512
U.a.isabellinus	U	WML	1963.73.34	Kashmir, India	31.727	75.512
U.a.isabellinus	M	WML	23.5.74.1	Kashmir, India	31.727	75.512
U.a.isabellinus	F	WML	23.5.74.2	Kashmir, India	31.727	75.512
U.a.alascensis	M	AMNH	100385	Rainy pass, confluence of R.styx&Sfork, Alaska, USA	62.084	-152.717
U.a.alascensis	F	AMNH	137226	White river,15mi E Russell Glacier, Alaska, USA	60.08	-142.098
U.a.alascensis	M	AMNH	167874	Tokichita glacier,125 m NW Anchorage, Alaska, USA	62.369	-151.42
U.a.alascensis	M	AMNH	212871	Upper Yentna river, Alaska, USA	62.183	-151.633
U.a.alascensis	M	AMNH	212872	Hicks creak, about 97 mi Glenn Highway, Alaska, USA	61.809	-147.871
U.a.alascensis	M	AMNH	212873	Upper Yentna river, Alaska, USA	62.183	-151.633
U.a.alascensis	F	AMNH	212874	Deadman Laka, 20mi N Susitna,N of Fog lakes, Alaska, USA	62.783	-148.489
U.a.alascensis	F	AMNH	90793	Port Moller,	56.005	-160.56

				Alaska, USA		
U.americanus	U	WML	11.2.67.2	Unknown		
U.americanus	U	WML	11.2.67.3	North America 4mi NE Archbold biological Station, Highlands Co.		
U.americanus	M	AMNH	144885	Baygall swamp, Florida, USA	27.34	-81.34
U.americanus	M	AMNH	167876	Jackson's stole, Wyoming, USA	43.479	-110.762
U.americanus	U	WML	1963.173.43	Wisconsin, USA	43.784	-88.787
U.americanus	U	WML	1981.2081	Unknown		
U.americanus	M	AMNH	215219	Indian lake, New York, USA	43.782	-74.265
U.americanus	U	WML	29.6.68.1	Unknown		
U.americanus	F	AMNH	49	Ponpon, South Carolina, USA	32.777	-80.47
U.americanus	F	WML	7.3.78.2	Colorado, USA	39.55	-105.782
U.maritimus	U	WML	1963.173.41	Unknown		
U.maritimus	U	WML	1963.173.56	Unknown		
U.maritimus	U	WML	1981.2047	Unknown		
U.thibetanus	M	AMNH	114544	Hpawshi hka,7400ft, Myanmar	26.429	98.506
U.thibetanus	U	WML	1963.173.146	Unknown		
U.thibetanus	U	WML	1963.173.45	Unknown		
U.thibetanus	U	AMNH	45293	Chihli province (Hebei), Tunq-linq, China	39.435	114.946
U.thibetanus	U	AMNH	57076	Unknown		
U.thibetanus	M	AMNH	84389	Chunqan Hsien,Fukien province, China	25.954	118.364
U.thibetanus	M	AMNH	87411	Indochina	19.227	98.84
U.arctos	U	ZMCU	1894	Norway	58.631	8.856
U.arctos	U	ZMCU	1895	Norway	58.631	8.856
U.arctos	U	ZMCU	1896	Norway	58.631	8.856
U.arctos	U	ZMCU	1897	Norway	58.631	8.856
U.arctos	U	ZMCU	1900	Norway	58.631	8.856
U.arctos	U	ZMCU	1902	Norway	58.631	8.856
U.arctos	U	ZMCU	1903	Norway	58.631	8.856
U.arctos	U	ZMCU	1904	Norway	58.631	8.856
U.arctos	F	ZMCU	2491	Loimola, Finland	60.85	23.059
U.arctos	U	ZMCU	569	Naes Ironworks, Norway	58.631	8.856
U.arctos	U	ZMCU	570	Naes Ironworks, Norway	58.631	8.856
U.arctos	U	ZMCU	571	Naes Ironworks, Norway	58.631	8.856
U.arctos	U	ZMCU	573	Naes Ironworks,	58.631	8.856

				Norway		
U.arctos	U	ZMCU	574	Naes Ironworks, Norway	58.631	8.856
U.arctos	U	ZMCU	575	Naes Ironworks, Norway	58.631	8.856
U.arctos	U	ZMCU	576	Naes Ironworks, Norway	58.631	8.856
U.arctos	U	ZMCU	577	Naes Ironworks, Norway	58.631	8.856
U.a.syriacus	M	ZMCU	2979	Zoo		

Appendix 2. List of bioclimatic variables extracted for each specimen locality.

BIO1 = Annual Mean Temperature

BIO2 = Mean Diurnal Range (Mean of monthly (max temp - min temp))

BIO3 = Isothermality (BIO2/BIO7) (* 100)

BIO4 = Temperature Seasonality (standard deviation *100)

BIO5 = Max Temperature of Warmest Month

BIO6 = Min Temperature of Coldest Month

BIO7 = Temperature Annual Range (BIO5-BIO6)

BIO8 = Mean Temperature of Wettest Quarter

BIO9 = Mean Temperature of Driest Quarter

BIO10 = Mean Temperature of Warmest Quarter

BIO11 = Mean Temperature of Coldest Quarter

BIO12 = Annual Precipitation

BIO13 = Precipitation of Wettest Month

BIO14 = Precipitation of Driest Month

BIO15 = Precipitation Seasonality (Coefficient of Variation)

BIO16 = Precipitation of Wettest Quarter

BIO17 = Precipitation of Driest Quarter

BIO18 = Precipitation of Warmest Quarter

BIO19 = Precipitation of Coldest Quarter
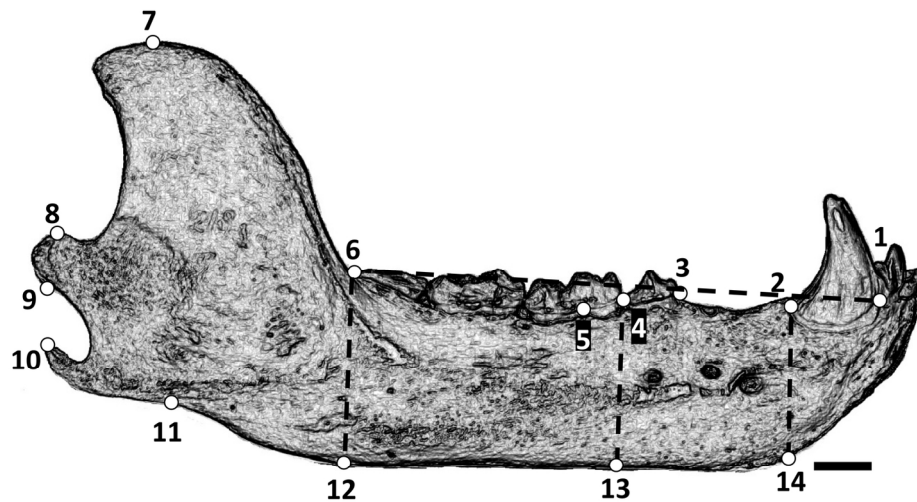
Fig. 1. Landmark configuration on a mandibular outline of brown bear (Ursus arctos). Landmark definitions
are as follow: 1 anterior tip of canine alveolus; 2 posterior tip of the canine alveolus; 3 anterior tip of
alveolar premolar 4 (p4) edge; 5 anterior tip of the alveolar lower carnassial (m1) edge; 6 lower alveolar
edge defining m1 slicing area; 7 posterior edge of m3 alveolus; 7 most superior tip of the coronoid process;
8 and 9 anterior and posterior
tips of mandibular condyle in lateral view; 10 posterior tip of the angular process; 11 ventral extreme of the
angular process; 12, 13 and 14 are projection of landmarks 2, 4 and 12 perpendicular to the line 1-6

150x88mm (300 x 300 DPI)
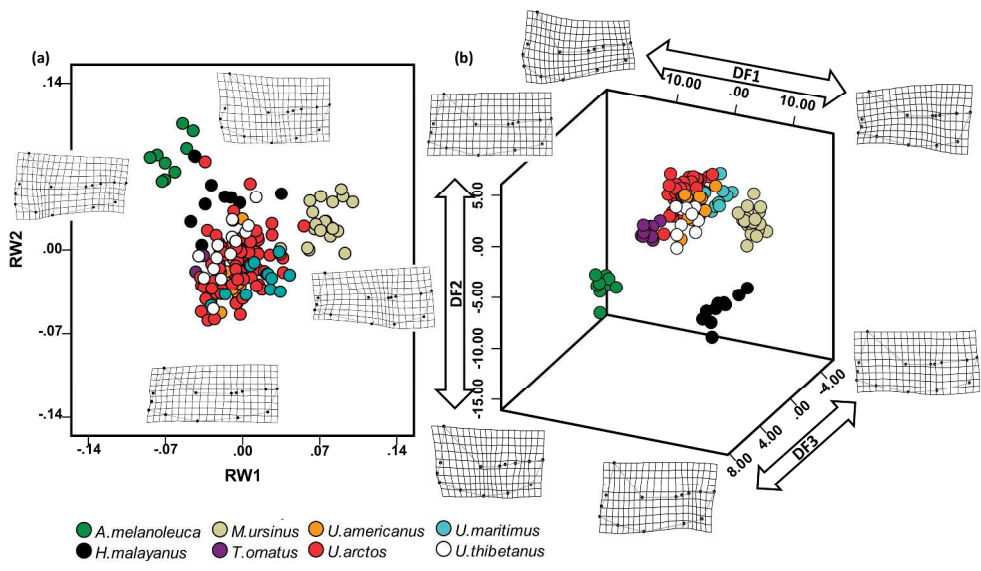
Fig. 2. Scatterplot of: (a) the first two Relative Warp axes obtained from shape variables. Deformation grids at the onset of each axes show relative shape changes from the mean described by each RW vector, (b) the first three Discriminant Function vectors obtained from a combination of shape coordinates and size. Deformation grids at the onset of each DF axes were obtained by regressing original shape coordinates vs DF vector scores. Label colours according to species
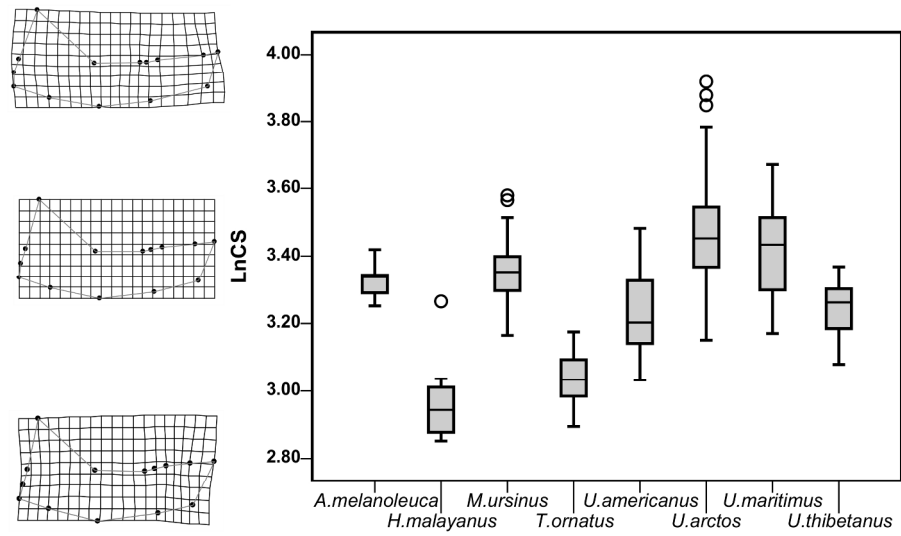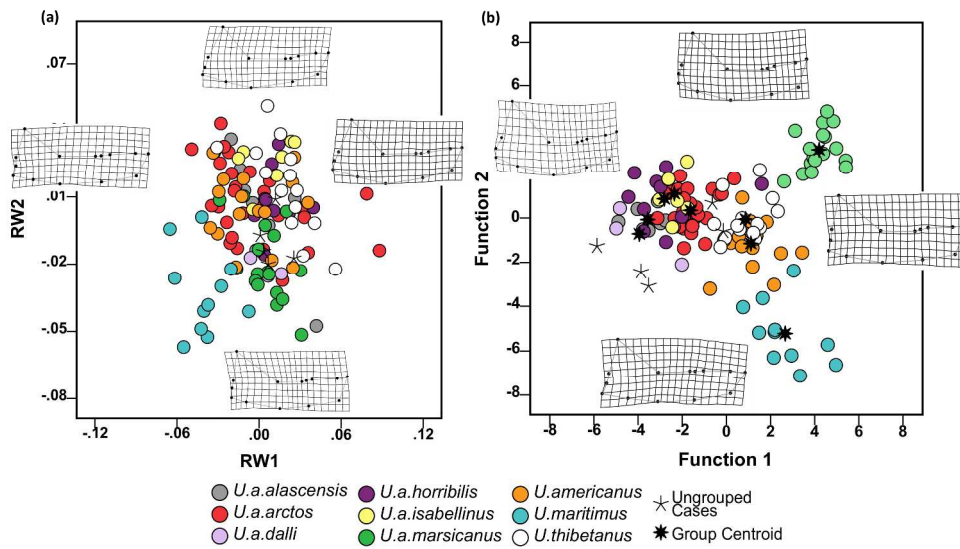
255x149mm (300 x 300 DPI)

Fig. 3. Mandible shape deformation related to size from the smallest (H. malayanus) to the largest (U. arctos) bear species with a box plot showing differences in natural log transformed centroid size ursid species
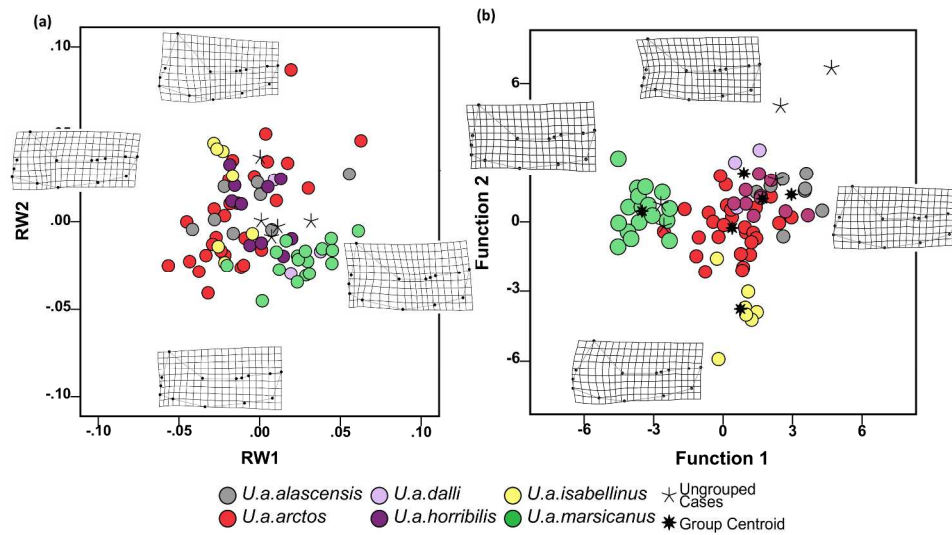
238x146mm (300 x 300 DPI)

Fig. 4. Scatterplot of: (a) the first two Relative Warp axes obtained from shape variables. Deformation grids at the onset of each axes show relative shape changes from the mean described by each RW vector; (b) the first two Discriminant Function vectors obtained from a combination of shape coordinates and size. Deformation grids at the onset of each DF axes were obtained by regressing original shape coordinates vs DF vector scores. Label colours according to Ursus species and subspecies of U. arctos

255x156mm (300 x 300 DPI)

Fig. 5. Scatterplot of: (a) the first two Relative Warp axes obtained from shape variables. Deformation grids at the onset of each axes show relative shape changes from the mean described by each RW vector: (b) the first two Discriminant Function vectors obtained from a combination of shape coordinates and size. Deformation grids at the onset of each DF axes were obtained by regressing original shape coordinates vs DF vector scores. Label colours according to subspecies of U. arctos

254x147mm (300 x 300 DPI)
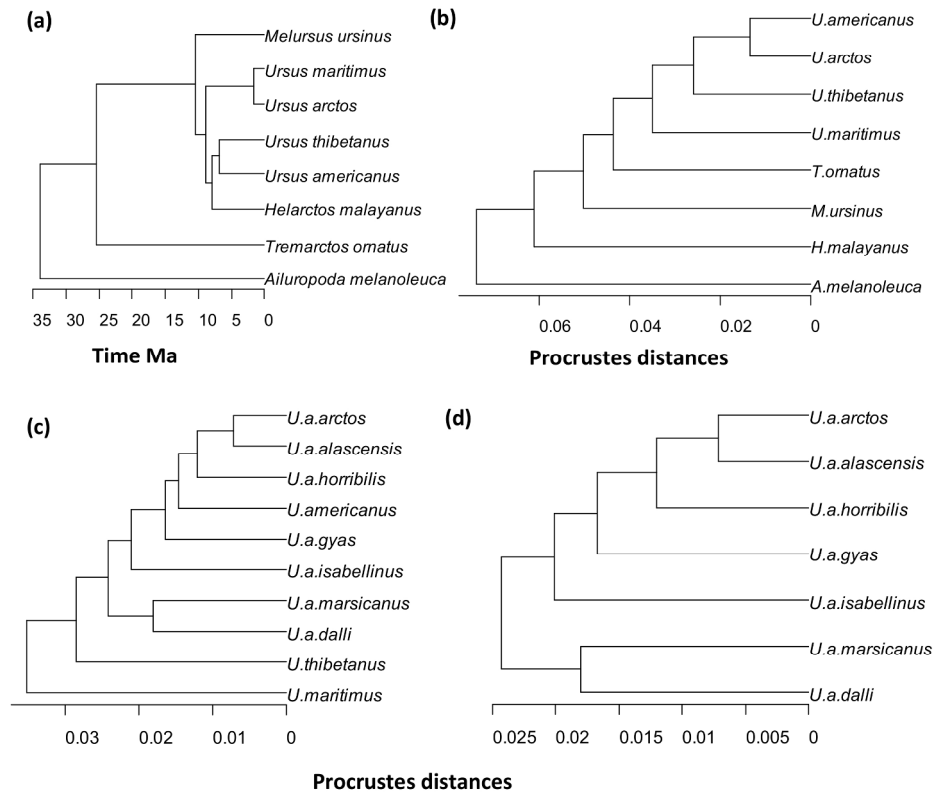
Fig. 6. Phylogenetic hypothesis for extant bears based on molecular data (a) followed by UPGMA trees of Procrustes distances from mandible shape data inclusive of: (b) all eight species of bears, (c) Ursus species and U. arctos subspecies, and (d) U. arctos subspecies only
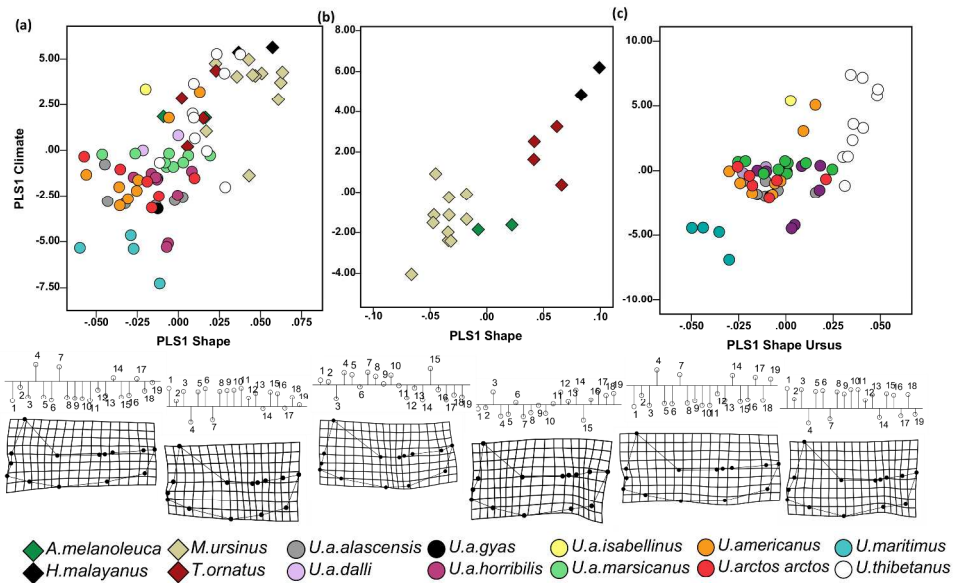
240x216mm (300 x 300 DPI)

Fig. 7. Scatterplot of the first pair of Partial Least Squares vectors for: (a) all Ursidae; (b) all tropical ursid species; (c) all Ursus spp. Variable and shape vectors are given respectively along the ordinate and the abscissa. Deformation grids show shape changes in correspondence of the extremes the first axis while variables profiles give the estimate of the standardized scores of each variable as vertical lines extending from a horizontal axis corresponding to the mean
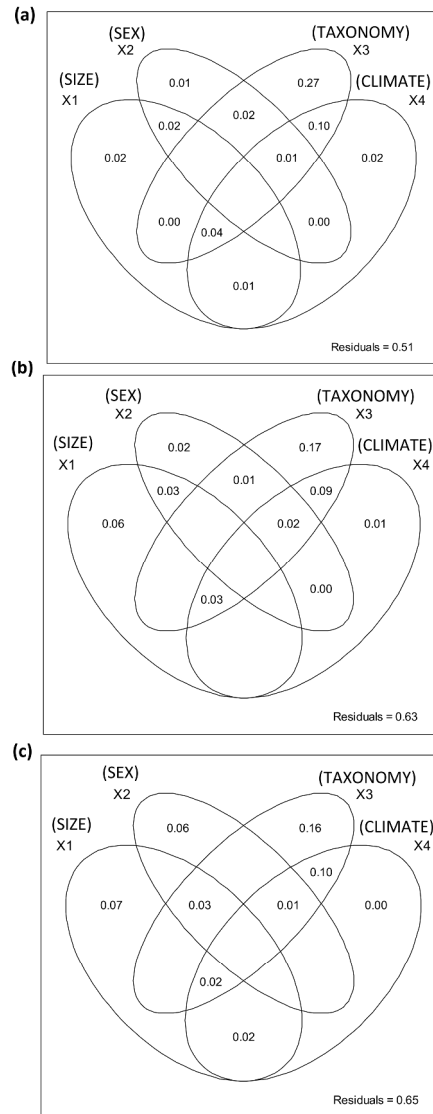
279x168mm (300 x 300 DPI)

Fig. 8. Schematic depiction of the factors size, sex, taxonomy and climate included in variation partition analysis meant to illustrate their individual contribution and relative interaction to mandible shape variance. We used a sample of mandibles with geographic locations of (a) all Ursidae (N = 66); (b) all Ursus spp. (N = 52); (c) all U. arctos (N = 36)

261x613mm (300 x 300 DPI)